J. Am. Soc. Mass Spectrom. (2012) 23:213–224
DOI: 10.1007/s13361-011-0274-x

RESEARCH ARTICLE

Compelling Advantages of Negative Ion Mode Detection in High-Mass MALDI-MS for Homomeric Protein Complexes

Stefanie Mädler, Konstantin Barylyuk, Elisabetta Boeri Erba, Robert J. Nieckarz, Renato Zenobi

Department of Chemistry and Applied Biosciences, ETH Zurich, 8093 Zurich, Switzerland

Abstract

Chemical cross-linking in combination with high-mass MALDI mass spectrometry allows for the rapid identification of interactions and determination of the complex stoichiometry of noncovalent protein–protein interactions. As the molecular weight of these complexes increases, the fraction of multiply charged species typically increases. In the case of homomeric complexes, signals from multiply charged multimers overlap with singly charged subunits. Remarkably, spectra recorded in negative ion mode show lower abundances of multiply charged species, lower background, higher reproducibility, and, thus, overall cleaner spectra compared with positive ion mode spectra. In this work, a dedicated high-mass detector was applied for measuring high-mass proteins (up to 200 kDa) by negative ion mode MALDI-MS. The influences of sample preparation and instrumental parameters were carefully investigated. Relative signal integrals of multiply charged anions were relatively independent of any of the examined parameters and could thus be approximated easily for the spectra of cross-linked complexes. For example, the fraction of doubly charged anions signals overlapping with the signals of singly charged subunits could be more precisely estimated than in positive ion mode. Sinapinic acid was found to be an excellent matrix for the analysis of proteins and cross-linked protein complexes in both ion modes. Our results suggest that negative ion mode data of chemically cross-linked protein complexes are complementary to positive ion mode data and can in some cases represent the solution phase situation better than positive ion mode.

Key words: Chemical cross-linking, NHS ester, MALDI-TOF-MS, Multiply charged ions

Introduction

A large number of known proteins exist in vivo as oligomeric species, many of which are homomeric complexes consisting of several subunits of the same protein [1]. In order to determine the oligomeric state and to provide kinetic and thermodynamic data, a number of analytical techniques have been applied, such as isothermal titration calorimetry, ultracentrifugation, or nuclear magnetic resonance spectroscopy. However, most of these methods are rather time-consuming, require a large amount of sample, and often do not provide any stoichiometric information. In contrast, mass spectrometric (MS) methods offer several advantages over traditional methods for the analysis of protein–protein interactions, such as high sensitivity, low sample consumption, and fast analysis time. Soft ionization techniques, such as electrospray ionization (ESI) or matrix-assisted laser desorption/ionization (MALDI), are capable of maintaining the primary structure of the proteins. A number of studies showed the potential of ESI-MS to investigate the stoichiometry, subunit assembly, and even binding strengths of noncovalent biomolecular complexes [2–4], but only few reports focused on native ESI to study homomeric polypeptide complexes in a qualitative and quantitative manner [5–7]. In contrast to ESI, the peaks in MALDI mass spectra are

Correspondence to: Renato Zenobi; *e-mail:* zenobi@org.chem.ethz.ch

Received: 5 August 2011
Revised: 4 October 2011
Accepted: 8 October 2011
Published online: 1 December 2011

predominantly singly charged ions, which greatly simplifies data interpretation. To prevent complex dissociation during MALDI analysis, chemical cross-linking has been applied prior to MS analysis for rapid identification of interactions and determination of complex stoichiometry [8, 9].

Singly charged protein complex ions generate signals at very high mass-to-charge ratios (*m/z*) in MALDI experiments. Novel detector technologies allow measurements of analytes up to several MDa and provide the basis for studying immunocomplexes and protein multimers [10, 11]. With increasing protein mass, signals corresponding to multiply charged species emerge in the MALDI mass spectra. For homomeric protein complexes, an overlap of these with complex subunits occurs. In the simplest case of a protein dimer, the singly charged monomer is detected at the same *m/z* as the doubly charged dimer. In order to apply chemical cross-linking and MALDI-MS for the analyses of homomeric protein complexes, the reduction of multiply charged species is desirable. Previous research on the charge distribution focused on the opposite, namely the search for parameters to *increase* the number of multiply charged cations since higher charge states open the way to extend the accessible mass range of instruments with limited *m/z* range and enhance the fragmentation for structural investigations. Elevated gas pressure in the source region [12, 13] laser powers just above the threshold [12], addition of glycerol [14], electrospray-deposition onto a matrix layer [15], low abundance of photoelectrons by thick sample layers or deposition on an "electron-free" surface [16–18], and matrices with low proton affinity (such as alpha-cyano-4-hydroxycinnamic acid (CHCA)) [19], favor the presence of higher charge states for polypeptides.

In order to reduce the fraction of multiply charged ions, the use of negative ion mode detection showed very promising results [20–22]. The reason for this is not known. The detection of large biomolecules is not typically performed in negative ion mode and, as such, a smaller amount of attention has been given to anion production mechanisms.

The following paragraphs review both positive and negative ion production mechanisms and ion yields postulated in the literature. Upon laser irradiation, ions of both polarities are generated. The fraction of negative ions has been reported controversially. In an early study, very similar laser threshold fluences for the production of positive and negative ions were reported [23]. However, anion signals typically had lower intensities than cations signals. Dashtiev et al. observed 4-fold lower signal intensities in negative ion mode than in positive mode on a commercial instrument for CsI [24]. The discrimination between the two polarities was speculated to be either due to the system configuration, which was optimized for the detection of cations, or due to the post-acceleration experienced by positively charged ions in front of the detector. Measurements on a dual-polarity TOF instrument, which simultaneously detects ions of both polarities with equal efficiency, revealed comparable signal intensities for positively and negatively charged ions of mid-mass polypeptides [21].

Two main models have been developed to explain ion formation during MALDI: (1) the cluster ionization model developed by the Karas group [20, 25], and (2) the gas-phase proton-transfer model [26], which has been carefully investigated by our group. For the latter mechanism, Knochenmuss introduced a quantitative rate equation model and estimated the positive to negative ion ratios for different instrumental and sample parameters using differential equations [27–29]. Depending on the free energies for the secondary ionization reaction, sample and instrumental parameters influence the ratio of positive to negative ion yields. However, when assuming similar free energies for positive and negative ions, the ratio is about 1.

Different ionization mechanisms for positive and negative ions have been suggested [30, 31]. A very recent paper presented a mechanism that unifies the cluster ionization and the gas-phase proton-transfer model [30]. For positive ions, instrumental and sample parameters dictate which model dominates in the ion formation process, whereas negative ions were assumed to form exclusively via the gas-phase proton-transfer model. One reason might be the presence of photoelectrons released when using stainless steel substrates [31].

The effects of different parameters on the distribution of negatively charged species have not been investigated so far. Here, we studied a number of proteins with regard to the abundance of multiply charged anions and cations. Additionally, we examined the effects of pertinent sample preparation and instrumental parameters on the charge distribution in both ion modes applying an ion-to-ion conversion detector (ICD), which allows for the detection of high-mass ions up to 1.5 MDa with high sensitivity [32]. The possibility of saturation is greatly reduced by adding capacitance buffers to the last electrodes of the used discrete dynode secondary electron multiplier. Another advantage of the ICD compared with conventional detectors is the lack of detector bias for ions of different polarities. With the ICD, both anions and cations experience a post-acceleration in front of the conversion dynode, which is operated at a potential of −20 kV in positive ion mode and +15 kV in negative ion mode, while keeping the acceleration potential in the source at +20 kV or −20 kV, respectively. Consequently, discrimination against negative ions due to a lower velocity close to the detector is *not* an issue for the high-mass detector.

Several chemically cross-linked homomeric protein complexes were investigated in order to compare the MALDI mass spectra in both ion modes. As chemical cross-linkers, highly amine-reactive homobifunctional *N*-hydroxy succinimide (NHS) or azabenzotriazole esters were used to stabilize the complex subunits covalently [33, 34].

Most applications of negative ion mode MALDI-MS focus on relatively small acidic compounds such as metabolites [35], oligonucleotides [36], or phosphopeptides [37]. This work intends to reveal the chances of detecting negatively charged protein and cross-linked protein complex ions and clearly work out the advantages of this detection

mode for the analysis of noncovalent complexes with MALDI-MS.

Materials and Methods

Albumin (BSA, bovine serum), aldolase (rabbit muscle), β-lactoglobulin (bovine milk), concanavalin A (*Canavalia ensiformis*), glutathione-S-transferase (GST, *Schistosoma japonicum*), glyceraldehyde-3-phosphate dehydrogenase (GADPH, rabbit muscle), immunoglobulin G (IgG, bovine serum), lysozyme (hen egg), myoglobin (horse heart), phosphorylase b (rabbit muscle), pyruvate kinase (rabbit muscle), ribonuclease A (bovine pancreas), trypsinogen (bovine pancreas), acetonitrile, and sinapinic acid (SA) were obtained from Sigma-Aldrich Chemie GmbH (Buchs, Switzerland). Citrate synthase (CS, *Escherichia coli*) was purchased from Megazyme (Bray, Co. Wicklow, Ireland), and creatine kinase (rabbit) from Roche (Basel, Switzerland). Trifluoroacetic acid (TFA) was obtained from Acros Organics (Thermo Fisher Scientific, Geel, Belgium).

The cross-linkers disuccinimidyl suberate (DSS) and bis (sulfosuccinimidyl) suberate (BS^3) were obtained from Pierce Protein Research Products (Thermo Fisher Scientific, Rockford, IL, USA). The cross-linker 1,1′-(suberoyldioxy)bis azabenzotriazole (SBAT) was synthesized in-house [34]. All commercial solvents and reagents were obtained in the highest available purity and used without additional purification.

Protein Preparation

Protein samples provided in ammonium buffers (citrate synthase, pyruvate kinase, and aldolase) were ultrafiltered repeatedly using Vivaspin 500 columns (molecular weight cut-off 10 or 50 kDa; Sartorius, Göttingen, Germany) and ultrapure water or 10 mM phosphate buffer (NaH_2PO_4–Na_2HPO_4, pH 8). The remaining protein samples were either dissolved in ultrapure water for general tests or phosphate buffer for cross-linking experiments. Protein concentrations were estimated by UV absorption at 280 nm using a small volume spectrophotometer (NanoDrop 1000; Thermo Fisher Scientific, Wilmington, MA, USA). The stock solutions were diluted with the respective buffer to concentrations indicated for the different experiments.

Cross-linking conditions, such as protein concentration, type of cross-linker and molar excess, were individually optimized for citrate synthase, aldolase, GST, and GADPH to obtain maximum yields of specific complexes. Typically, 10 µL of the protein solutions at 5 to 40 µM concentration were mixed with a 40- to 100-fold molar excess of DSS, BS^3 or SBAT dissolved in dimethylformamide (DSS, SBAT) or water (BS^3) in a 10/1 (vol/vol) ratio and incubated for 0.5 to 2 h at room temperature. Ten µL of protein solution plus 1 µL of dimethylformamide was used as a control for experiments with DSS and SBAT. If needed, the reaction mixtures were diluted with water prior to mass spectrometric analysis.

Mass Spectrometric Detection

A commercial instrument (MALDI TOF/TOF 4800 Plus analyzer; AB SCIEX, Darmstadt, Germany) equipped with a previously described high-mass detector (HM2 Tuvo; CovalX AG, Zurich, Switzerland) was employed [32]. Measurements were performed in both linear positive and negative ion modes. Experimental conditions (i.e., lens voltages, DE times) were optimized for positive ion mode. Exactly the same absolute voltage settings (with opposite polarity) were used for negative ion mode (when separately optimizing the settings for negative ion mode, the resulting spectra were very similar). Desorption/ionization was initiated by using a frequency-tripled Nd:YAG laser (355 nm) with different pulse energies. Each mass spectrum was the average of typically 1000 to 3000 laser shots obtained automatically at random sample positions. SA was used as a matrix, dissolved at 10 mg/mL in water/acetonitrile/TFA (49.95/49.95/0.1, vol/vol/vol). Among a large number of tested matrices including dihydroxybenzoic acid (DHB), α-cyano-4-hydroxycinnamic acid (CHCA), 2,6-dihydroxyacetophenone (DHAP), and 6-aza-2-thiothymine (ATT), SA produced spectra with the best compromise between narrow peak widths and low detection limit in both positive and negative ion modes. The ion yield in both detection modes is known to neither depend on the number of acidic and basic amino acids present nor on the gas-phase basicity/acidity of the matrix [24, 38]. The use of a basic matrix such as ATT did not enhance anion signal intensities, but yielded detection efficiencies comparable to SA.

Surprisingly, the addition of TFA to the matrix solvent improved the spectral quality in both ion modes. We assume that the acidic conditions provided by TFA improve the crystallization of the organic matrix molecules and incorporation of analytes. The samples were directly mixed with the matrix in a 1/1 (vol/vol) ratio. One µL of the mixture was spotted on a stainless steel plate and allowed to dry under ambient conditions. All mass spectra were baseline-corrected and smoothed using a Savitzky-Golay algorithm. Peak integrals were calculated using dedicated software (ComplexTracker; CovalX) and an average of typically five spectra was used for data interpretation.

Results and Discussion

High-Mass MALDI-MS Detection of Proteins in Negative Ion Mode

To the authors' knowledge, high-mass detectors capable of detecting ions up to several 100 kDa have never been employed before for measuring high-mass proteins in negative ion mode. Compared with positive ion mode data, negative ion high-mass MALDI spectra on our setup show comparable resolution, lower background levels, smaller signals of multiply charged species, and higher reproducibility, which results in generally "cleaner" spectra. Typical spectra for IgG of the same spot series with the same laser

power in both ion modes are given in Figure 1. In order to obtain similar signal-to-noise ratios, a slightly higher laser power is necessary for negative ion mode. Since the same laser power was used for both spectra, the anion spectrum has a higher noise level, but also a lower intensity of the nonspecific dimer peaks. In negative ion mode, the limit of detection is on the orders of tens of femtomoles for IgG, about two to three times worse than in positive ion mode using dried-droplet sample preparation, SA as a matrix, and a commercial instrument. The absolute signal intensities of protein anions, as seen from the count values of the y scales in Figure 1, are generally several orders of magnitude lower than cations. Although the hardware and parameter settings used in commercial instruments might favor higher signal intensities for cations, this result supports the notion of different production mechanisms for positive and negative ions, which can lead to substantially lower yields for anions than for cations. Taking into account the proposed dominance of the gas-phase proton-transfer model in negative ion mode [30], use of a basic matrix would increase signal intensities of anions. However, none of the tested basic matrices (such as ATT) or less acidic matrices (such as DHAP) yielded higher signal intensities than SA, which was eventually used for all measurements. We suggest that the use of a basic matrix that optimally incorporates high-mass proteins might increase anion signal intensities. However, no basic matrix that fulfils this prerequisite has been found yet.

Another obvious characteristic of negative ion mode spectra was the lower fraction of multiply charged ions compared with singly charged ions. The triply charged species, for example, which was abundant in positive ion mode, could hardly be observed in negative ion mode. In order to confirm this observation, MALDI mass spectra of a number of proteins were recorded in both ion modes to compare their charge distribution: aldolase, β-lactoglobulin, concanavalin A, glutathione-S-transferase, glyceraldehyde-3-phosphate dehydrogenase, immunoglobulin G (IgG), lysozyme, myoglobin, phosphorylase b, pyruvate kinase, ribonuclease A, trypsinogen, citrate synthase, and creatine kinase. These proteins cover a molecular weight range from 13.7 kDa (ribonuclease A) to about 150 kDa (IgG). In these experiments, the laser power was optimized to yield optimum signal-to-noise ratios and resolving power. Therefore, a higher energy was applied in negative ion mode (5000 a.u. compared with 4450 a.u. in positive ion mode). The signal integrals of doubly charged ions normalized to the integrals of singly charged monomeric species were plotted against the molecular weight of the proteins (Figure 2). For all investigated proteins, doubly charged anions were far less abundant than doubly charged cations. These results were confirmed using a second MALDI-TOF instrument retrofitted with an ICD (Reflex III; Bruker, data not shown).

The fraction of doubly charged cations increased significantly with the molecular weight of the analytes. Minor amounts of triply charged cations could be detected for almost all proteins; their intensity increased with increasing molecular weight as well. The resulting curve suggests an empirical correlation with a power law. The dependence of the fraction of doubly charged cations can be expressed as $y = A \cdot M^B$, where M is the molecular weight of the protein, y

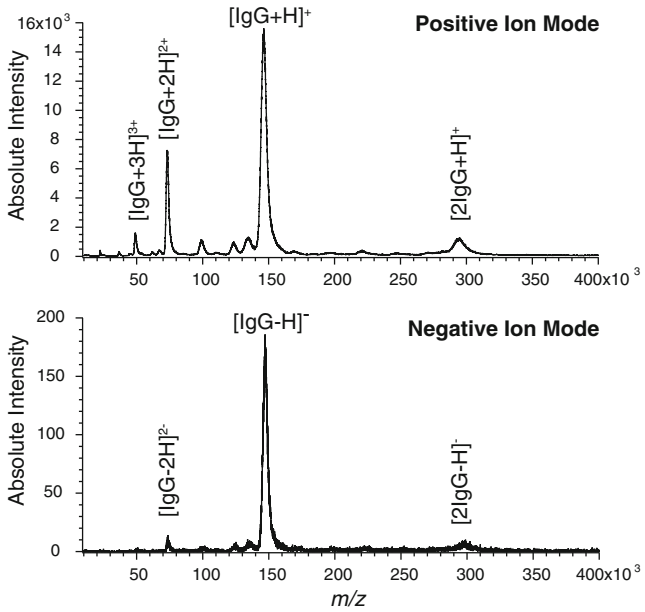

Figure 1. Typical MALDI mass spectra of IgG in positive and negative ion mode (laser power of 4450 a.u.) measured with SA as matrix. IgG was kept in an aqueous solution at a concentration of 1 μM prior to spotting onto the MALDI plate

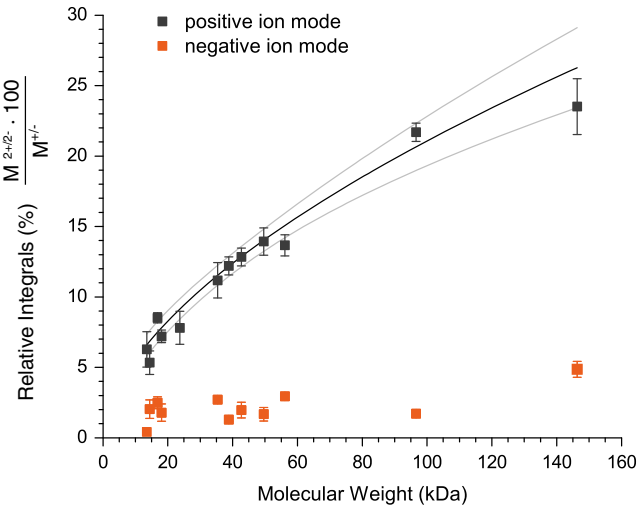

Figure 2. Comparison of relative intensities of doubly charged ions for a number of proteins derived from aqueous solutions at a concentration of 1 μM in positive and 2 μM in negative ion mode using an optimized laser power of 4450 a.u. (positive) and 5000 a.u. (negative) using SA as matrix. Error bars correspond to the standard deviations of at least five replicate measurements. The data were fitted with the equation $y = A \cdot M^B$. The fitting curve is shown in black. The grey lines indicate the 95% confidence interval

the integral ratio of doubly charged to singly charged monomer peaks. From a fit, we found $A=1.46\pm0.21$ and $B=0.58\pm0.04$ with an R^2 value of 0.954. The resulting "calibration" curve could be used to predict and estimate the contribution of relative signal intensities of doubly charged ions in MALDI mass spectra of protein complexes. For ESI-MS, the relationship between the size of a molecule and its charge state distribution has been investigated as well. Kaltashov and Mohimen could successfully fit the average charge state of various "natively" electrosprayed proteins as a function of the surface area of the proteins using a similar equation [39]. However, no correlation of the average charge state with the molecular weight was found in that work. In contrast, van Breukelen et al. introduced the equation $Z_R=0.078\ M^{0.5}$ that allows the estimation of the average charge state Z_R of a protein based on its molecular weight M [40]. The observed exponent is very similar to the one found here, although some difference between the MALDI and the ESI-MS data is expected since in this work the fraction of doubly charged ions, as opposed to the average charge state, was used.

For our experiments in negative ion mode, the molecular weight of the proteins influenced their charge distribution only to a minor degree. The fraction of doubly charged anions typically stayed fairly constant, between 1% and 5% (Figure 2). Measurements with lower laser power in negative mode yielded slightly higher ratios of doubly charged species, but resulted in a similar trend. No obvious dependence of the negative ion data on molecular weight was observed.

The formation of multiply charged ions could result from incomplete neutralization (in the case of the cluster ionization model) or from several subsequent protonation/deprotonation reactions (for the gas-phase proton-transfer model). Multiply charged cations are the result of incomplete neutralization with negatively charged matrix ions or electrons in the cluster ionization model [20, 25, 30]. For the gas-phase proton-transfer model, the number of added protons depends mainly on thermodynamic considerations and thus on the proton affinity of analyte and matrix [26, 41]. As discussed above, negative ions have been suggested to result exclusively from gas-phase charge or proton transfer reactions, in the simplest case deprotonation after gas-phase collisions with negatively charged matrix ions [30]. The gas-phase basicity of deprotonated matrix molecules is on the order of 1300 kJ/mol [42], whereas the gas-phase acidity of amino acids is on the order of 1400 kJ/mol [43]. Depending on the analyte, the abstraction of one or more protons from an analyte becomes an endergonic process. From a thermodynamic point of view, the formation of multiply charged ions seems less probable for anions than for cations.

Influence of Experimental Parameters on the Charge Distribution

With the aim of minimizing the intensity of undesired multiply charged ions and nonspecific adduct species in the analysis of homomeric complexes, the effect of sample preparation techniques and analysis parameters, such as sample concentration, laser power, and delayed extraction time were investigated in both polarities. The influence of two of the most important parameters, laser power and sample concentration, is depicted for IgG in Figure 3.

The results were obtained by averaging at least five measurements for each ion mode obtained from a minimum of eight different sample spots. The laser power was varied when targeting sample spots containing 500 fmol of IgG each. With increasing laser power (given in arbitrary units), the fraction of multiply charged ions decreased, whereas the number of nonspecific multimers increased slightly (Figure 3a, c). These results corroborate the measurements made with standard detectors in positive ion mode [22]. In positive ion mode (Figure 3a), reliable data were obtained between 3900 and 4500 a.u. For a laser power above 4500 a.u., the most intense peaks were truncated by the instrument software (data not shown). The peak integrals of multiply charged ions become more reproducible with increasing laser energy. In negative ion mode (Figure 3c), high precision data were obtained over a broad laser energy range with an average ratio of doubly charged versus singly charged species of 4.3% ± 1.0% and a relative dimer abundance of 2.9% ± 1.1%. In short, the relative peak intensities in positive ion mode were highly variable and dependent on the laser power, whereas only small variations occurred in the negative ion mode.

At low laser fluences, too little material might be released to maintain sufficient collisions before all reactions are complete. In this case, the mass spectrum reflects the results of primary rather than secondary ionization reactions [44]. Consequently, less charge reduction processes are expected to take place at low laser power and higher charge states would be observed [20]. At higher laser power, secondary reactions become dominant. Additionally, higher laser energies produce more photoelectrons from both the metal target and multiphoton ionization processes of the matrix and, thus, favor charge reduction for doubly charged cations in positive ion mode [16]. In negative ion mode, relevant protein signals were only observed at higher laser power.

IgG samples at concentrations between 0.2 and 5 μM were investigated with MALDI-MS using optimized laser powers (5000 a.u. in negative mode, 4100 a.u. in positive mode). The relative intensity of nonspecific dimers increased nonlinearly with increasing concentration for both ion modes (Figure 3b, d). This observation confirms previous results obtained with conventional MCP detectors [22, 45]. In positive ion mode only, a slight decrease of the doubly and triply charged ions was found with increasing concentration. Taking into account the large standard deviations for most data points, the trend is not statistically significant. Zhong and Zhao reported a much more pronounced, but similar tendency for a laboratory-built TOF instrument operated in positive ion mode, studying cytochrome *c* with SA as a matrix, silver as a substrate, and analyte concentrations between 0.6 and 1 μM [45]. In contrast, Tabet and coworkers

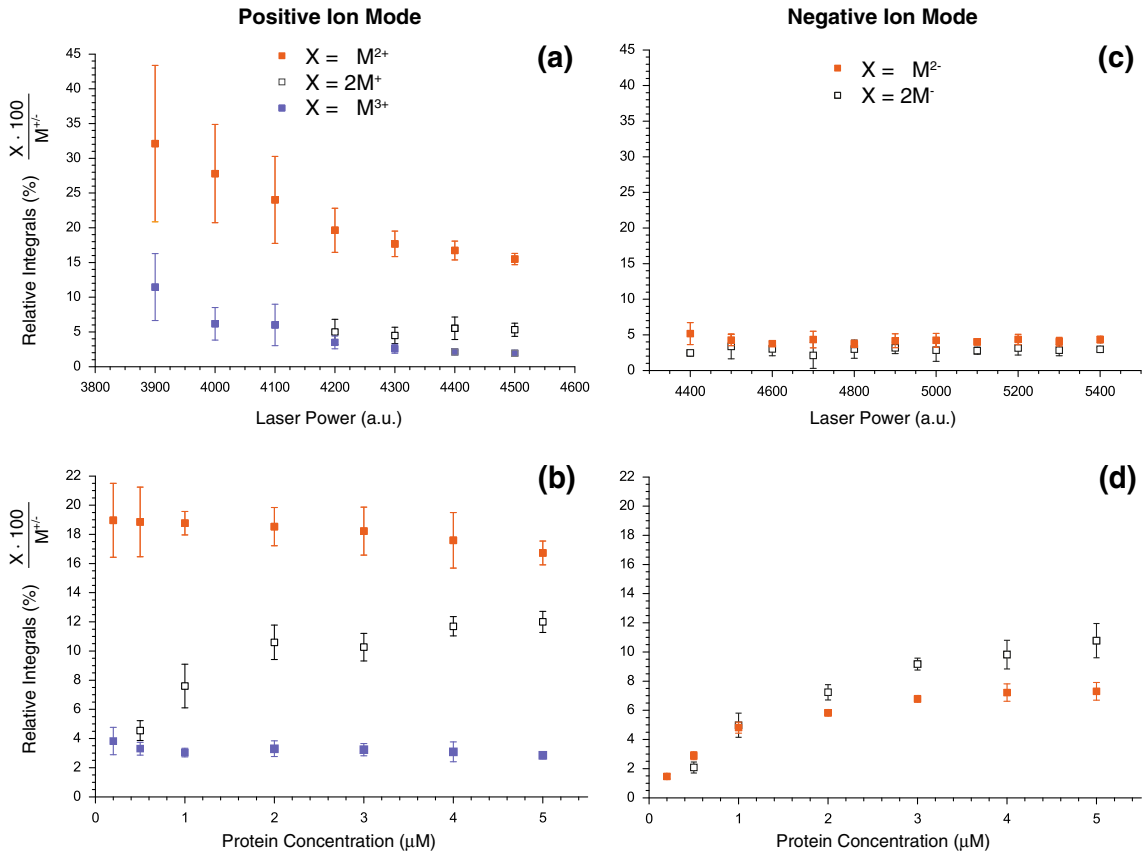

Figure 3. Effects of laser power **(a)**, **(c)** and protein concentration **(b)**, **(d)** on the intensity of multiply charged species and nonspecific adducts for IgG in both ion modes using SA as matrix. Error bars correspond to standard deviations of at least six replicate measurements

observed the opposite trend for BSA: lowering the analyte concentration led to a decrease of doubly charged ions in their experiments using a conventional microchannel plate (MCP) detector [22]. The MCP suffers from very low sensitivity for high-mass ions due to their low velocity and saturation effects caused by long channel recovery times [46–48]. With increasing sample concentration, more channels are blocked and the saturation effect of an MCP becomes more prominent. This artifact could lead to the increasing abundance of multiply charged ions with increasing concentration observed by Tabet and coworkers[22]. In our lab, data for BSA were measured with both detectors (MCP and ICD) over a similar concentration range (data not shown). The two detectors gave opposite results for multiply charged ions, i.e., an influence of the saturation effect mentioned above for the MCP detector is quite likely. The concentrations used by Zhong and Zhao were probably sufficiently low to avoid detector saturation.

For negative ion mode, increasing concentrations resulted in an increase of doubly charged ions with the ICD. Generally, negative ion mode data are more precise than positive ion mode data. The reasons for the different tendencies are not clear and will need further study. However, our results confirm different ionization/neutralization reactions for anions compared with cations.

The lowest relative intensity of unwanted species and, thus, the optimum condition for the purpose of this study was observed at the lowest concentration investigated, 0.2 µM, in negative ion mode. However, for cross-linking experiments with homomeric protein complexes with MALDI-MS, the spectral quality can deteriorate at low sample concentrations due to the presence of cross-linker molecules and their solvent. Thus, slightly higher concentrations are often necessary to obtain reasonable mass spectra. Choosing higher concentrations simplifies the quantitative determination of these unwanted species since their relative intensities only changed within a few percent over a broad concentration range during our experiments.

Typically, modern MALDI-TOF instruments feature delayed extraction, i.e., a ns to µs time lag before the analyte ions extraction pulse that helps to correct for differences in the initial velocity of desorbed species and to improve the focusing of arrival times at the detector. During this time period, the ablated material expands in the plume and undergoes a number of secondary reactions. The delayed extraction time was varied between 0 and 2000 ns and the corresponding MALDI mass spectra were recorded. For both ion modes, longer delay times reduced the relative intensity of multiply charged ions significantly, while a slight, albeit noticeable increase in the number of dimeric

species was also observed (data not shown). From this observation, it can be concluded that charge reduction processes taking place in the plume are likely to influence the charge distribution.

In summary, the use of a matrix with high proton affinity, long delayed extraction times, high sample concentration, and high laser power decreased the amount of multiply charged cations. However, the most efficient way to reduce the relative abundance of multiply charged ions was switching to negative ion mode detection. An additional advantage of negative ion mode measurements of proteins is the high reproducibility of the spectra and the relatively low dependence of the charge distribution on sample preparation parameters.

Application: Analysis of Chemically Cross-Linked Homomeric Protein Complexes

As discussed, chemical cross-linking in combination with MALDI-MS is a very powerful tool to probe the composition of homomeric protein assemblies. In order to determine the cross-linking yield, i.e., the fraction of chemically stabilized complex compared with the total amount of complex prior to addition of the cross-linker, it is necessary to obtain reliable mass spectrometric data. From the data, it should be possible to determine the fraction of multiply charged ions and nonspecific multimers, and the peak ratios should resemble the solution-phase composition as closely as possible. Based on the advantages of negative ion mode found in experiments with model proteins, we extended our work to investigate chemically cross-linked complexes. In Figure 4, the result of chemical cross-linking of homomeric protein complexes is illustrated for aldolase, which forms a tetramer. Without adding the stabilizing cross-linker, the monomeric species, its doubly charged ion, and nonspecific gas-phase adducts were detected (shown in grey). Again, the MALDI mass spectra using negative ion mode exhibited a significantly lower abundance of doubly charged monomer than in positive ion mode. After chemical cross-linking with BS^3, the stabilized tetrameric complex became the dominant species. The relative intensity of the doubly charged species measured for this complex corresponded surprisingly well with that for standard proteins shown in the calibration curve in Figure 2, although slightly different sample preparation conditions were used in this experiment. Thus, the data suggested a cross-linking efficiency close to 100%. For tetrameric aldolase from rabbit muscle, Tolan et al. estimated dissociation constants below 10^{-27} M^3 for the tetramer-monomer equilibrium and 10^{-12} M for the tetramer-dimer equilibrium using sedimentation equilibrium experiments [49]. In practical terms, this means that the protein exists exclusively as tetramer in its native state for concentrations above the nanomolar range. Consequently, the species distribution observed for this protein after chemical cross-linking and MALDI-MS agreed perfectly with the equilibrium state in solution in both ion modes.

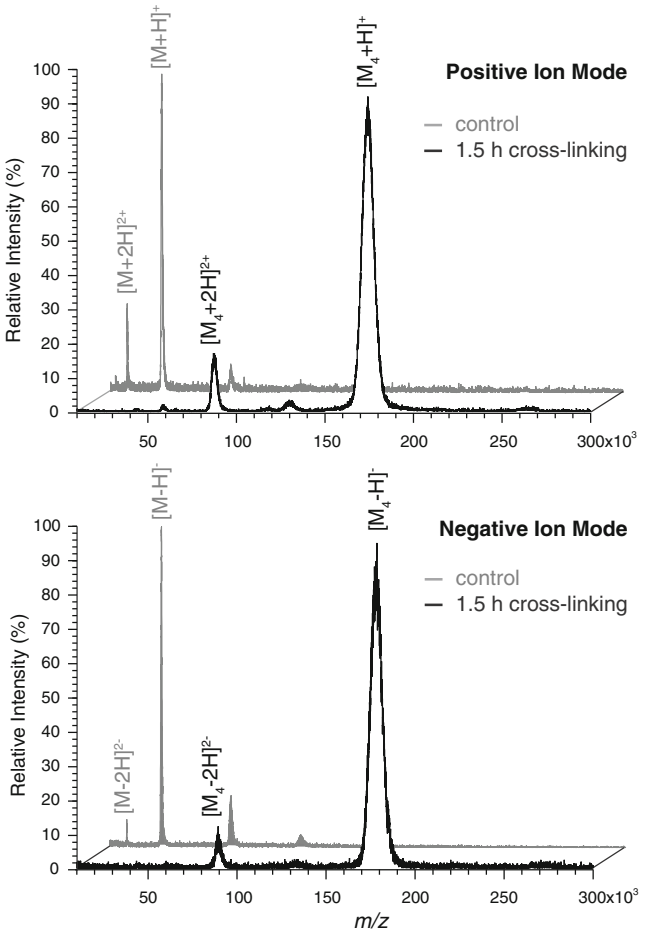

Figure 4. Comparison of MALDI mass spectra of cross-linked samples of tetrameric aldolase samples (20 μM monomer concentration, 10 mM phosphate buffer, pH 8, 40-fold molar excess of BS^3) after 1.5 h of cross-linking with mass spectra of aldolase prior to cross-linking (shown in grey) in positive and negative ion mode measured with SA as matrix

Upon reaction of the monomeric or oligomeric species with the cross-linker, a mass shift occurs. The mass increase caused by covalent addition of chemical cross-linkers depended strongly on the reaction time, type of cross-linker, its molar excess, the number of available reaction groups, and the pH value of the solution. It was typically several 1000 Da, much lower than the mass of a single subunit for all investigated protein complexes. Among the numerous reaction products, the presence of so-called "dead-end links", i.e. an amino acid modified with a cross-linker that is either hydrolyzed or still reactive at its second end, is very likely. If one considers an acylation of an amine group, a basic moiety is replaced by an acid functionality. In order to investigate if the higher number of acidic groups increased the fraction of multiply charged ions, control experiments with the model protein BSA were carried out. However, no significant changes in the intensity of multiply charged ions were observed after reaction with BS^3. Thus, chemical cross-

Table 1. Summary of the Investigated Proteins, with the Expected Stoichiometry Known from Literature, the Measured Complex Stoichiometry with MALDI-MS and Chemical Cross-linking, and the Yield of Cross-linked Complex for Both Ion Modes (Peak Integrals of the Respective Product with Highest Stoichiometry Relative to the Integral Sum of the Signals of Monomers and Oligomers). The Given Errors Correspond to Standard Deviations ($n \geq 3$). M, D, T, and H Refer to Monomer, Dimer, Tetramer, and Hexamer, Respectively; # Refers to the Number of Subunits in a Native Assembly of the Respective Protein

Protein name organism	K_D (Ref.)	Stoichiometry and complex yield	
		Negative mode	Positive mode
Aldolase *Rabbit muscle*	$<10^{-27}$ M^3 (M↔T) [49] 10^{-12} M (M↔D) [49]	4 (93 ± 1.2%)	4 (86 ± 2.3%)
GST *S. japonicum*	Not known, but probably in the nM range	2 (91 ± 1.1%)	2 (78 ± 2.1%)
GADPH *Rabbit muscle*	$5.0 \pm 0.2 \cdot 10^{-7}$ M (D↔T) [51]	4 (79.4 ± 6.4%)	2 (63.8 ± 2.4%) 4 (12.4 ± 1.5%)
Citrate synthase *E. coli*	$1.4 \pm 0.1 \cdot 10^{-11}$ M^2 (D↔H) [7]	2 (88.3 ± 4.2%) 4 (8.5 ± 2.0%)	2 (23.0 ± 5.6%) 4 (37.7 ± 4.9%) 6 (10.4 ± 8.7%)

linking is not likely to cause a dramatic shift in the charge distribution of the stabilized protein complexes.

Several proteins with homomeric quaternary structures ranging from 52 kDa (dimeric glutathione S-transferase) to 288 kDa (hexameric citrate synthase) were selected and subjected to chemical cross-linking with the cross-linkers SBAT, BS^3 and DSS, using a variety of concentrations and molar ratios. MALDI mass spectra of the cross-linked mixtures were recorded in both ion modes using the high-mass detector. The proteins chosen are listed in Table 1. The yields of the largest homomeric species were determined using the MALDI mass spectra and are also given in Table 1.

Figure 5 shows MALDI mass spectra of three other protein complexes in both ion modes. All positive and negative mode spectra shown for a protein complex were recorded from exactly the same sample spot. Glutathione S-transferase (GST) is known to have a very stable dimeric structure [50]. However, to the best of our knowledge, no K_D value has been reported. The MALDI mass spectra after cross-linking with BS^3 (Figure 5a, d) exhibit the dimer as the dominant species, with relative integrals of the dimer peak of 91% in negative and 78% in positive ion mode. Based on the calibration curve in Figure 2 and the molecular weight of the protein, 2% to 4% of the monomer signal in negative ion mode and 12% to 14% in positive ion mode must be attributed to the doubly charged dimer. Consequently, a cross-linking efficiency, i.e., the yield of stabilized dimer compared with the total amount of dimer in solution, between 90% and 96% was achieved. The negative ion mode delivered more direct and more reliable data for determining the cross-linking yields. Figure 5b and e depict the MALDI mass spectra recorded after chemical cross-linking of tetrameric GADPH. Early sedimentation equilibrium experiments at pH 7 in buffers with low ionic strength gave a dissociation constant of $5.0 \cdot 10^{-7}$ M for this system assuming a dissociation of the tetramer into dimers exclusively (Table 1)[51]. Based on this K_D value and a subunit concentration of 40 μM used for the cross-linking experiments with SBAT, the protein solution was expected to contain about 81% tetramer and 19% dimer. After chemical cross-linking, about 79% tetramer were detected in negative and 12% in positive ion mode. The negative ion mode data clearly reflected the predicted complex yields within error and allowed us to estimate a cross-linking yield of almost 100%, i.e., a covalent stabilization of almost all tetramers present in solution. In contrast, the spectrum recorded in positive ion mode from the same sample spot, mainly contained the dimeric species.

For citrate synthase, which forms a hexamer in its active form, Duckworth and coworkers assumed a pure dimer-hexamer equilibrium and determined its dissociation constant to be $1.4 \cdot 10^{-11}$ M^2 in 5 mM ammonium bicarbonate at pH 7.5 (Table 1) [7]. No monomeric species were detected under those conditions. On the basis of the reported K_D value, the product distribution in solution should be 35% hexamer and 64.5% dimer at a monomer subunit concentration of 15 μM used in this work. No monomers or complexes with other stoichiometries were expected to occur. As depicted in Figure 5c and f, the spectra obtained with MALDI-MS following chemical cross-linking (10 mM phosphate buffer at pH 8) differed from the reported ESI measurements mentioned above. When comparing the results, it has to be considered that Duckworth and coworkers used a recombinant protein expressed in their lab, whereas the citrate synthase we used was obtained from a commercial vendor. After chemical cross-linking, the dimer appeared in both polarities, while the hexamer appeared only in positive ion mode measurements for a small number of experiments. Assuming that the detected monomeric and tetrameric species are the result of incomplete cross-linking and do not reflect the equilibrium state composition of citrate synthase in solution, the sum of the peak integrals of tetrameric/hexameric species is slightly larger than that of the peaks corresponding to the monomeric/dimeric species (Table 4). The tetrameric/hexameric peaks are more abundant than expected from the K_D values obtained by Duckworth and coworkers [7]. Considering the relatively low subunit concentration used (15 μM), no unspecific cross-linking was expected to occur [52]. However, the measured relative abundances varied a lot, with standard deviations up to 100% and the spectra required severe baseline corrections prior to data interpretation.

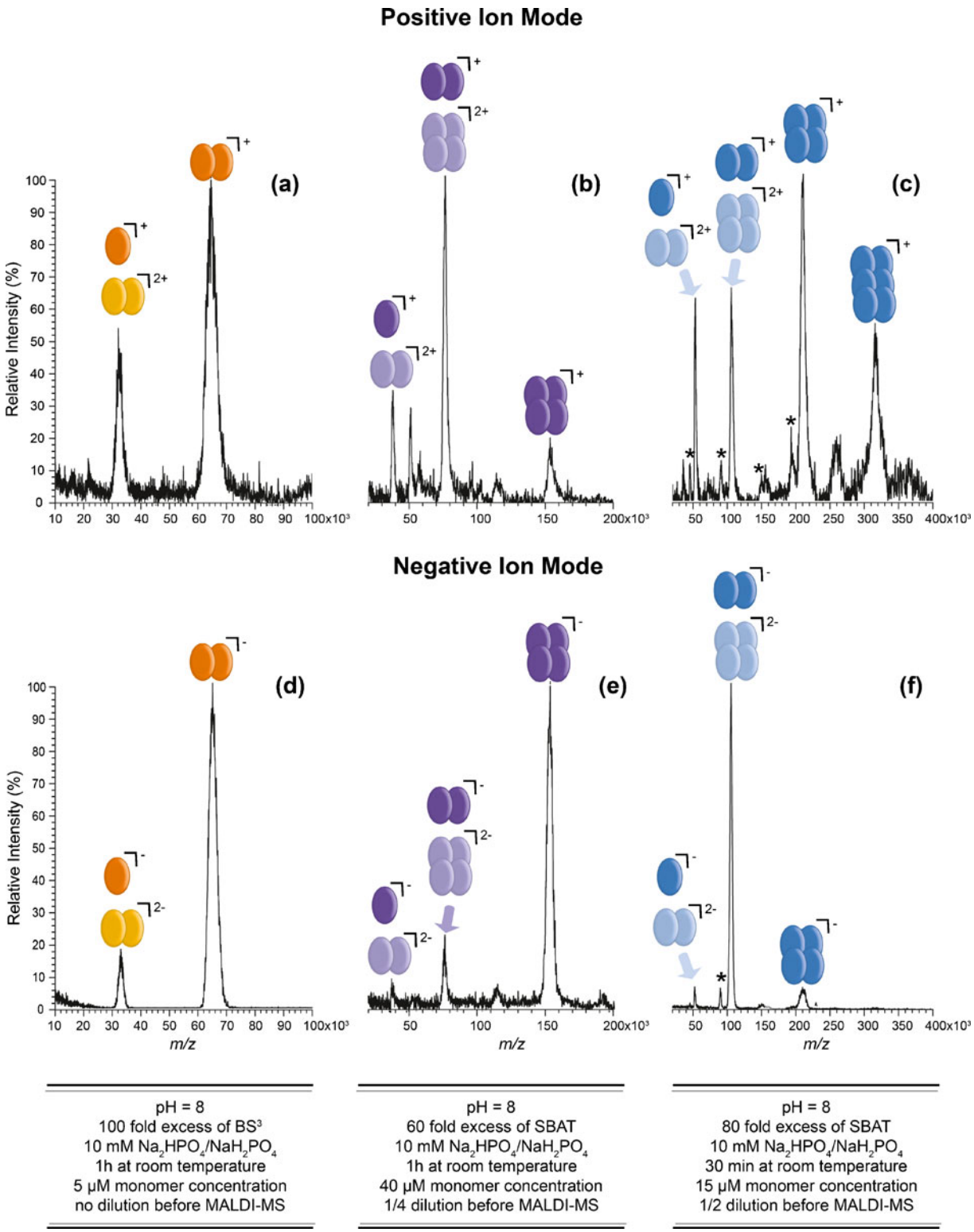

Figure 5. Comparison of MALDI mass spectra of cross-linked samples of homomeric protein complexes in positive **(a)**, **(b)**, **(c)** and negative ion mode **(d)**, **(e)**, **(f)** for GST **(a)**, **(d)**, GADPH **(b)**, **(e)**, and citrate synthase **(c)**, **(f)** measured with SA as matrix. The optimized cross-linking conditions are specified. In order to gain higher spectral quality, the samples were diluted before mixing with the matrix with the given dilution factor. The asterisks in the mass spectra of citrate synthase **(c)**, **(f)** correspond to peaks originating from an impurity. Whereas for GST positive and negative ion mode mass spectra yield comparable results in product distribution, the detected products differ significantly for citrate synthase and GADPH in both ion modes

In negative ion mode, the dominant signal was the cross-linked dimer at all tested conditions. A small amount of tetramer indicated the presence of a higher-order oligomeric complex, but no hexamers could be detected. Once again, the negative ion mode offered a lower baseline that did not require extensive data treatment. We believe that the protein was mainly stabilized in its dimeric assembly. The absence of hexamer peaks in negative ion mode could be the result of either incomplete cross-linking or the absence of hexameric complexes in solution. Based on the lower sensitivity observed for model proteins in negative ion mode, very small amounts of hexamer could be too low to be detected in negative ion mode.

In contrast, the positive ion mode data showed low spectral quality, very high intensity of the monomer peak, low reproducibility of the hexamer peak, and overrepresented tetrameric/hexameric ion signals. In other words, the positive ion mode spectrum probably can show artifacts, which do not resemble the solution-phase composition after chemical cross-linking. Consequently, the high intensity of the hexamer was possibly an artifact.

Other Possible Applications

All of the advantages of negative ion mode detection described above simplify spectra interpretation compared with positive ion mode detection. Due to the lower influence of sample preparation on the charge distribution, the fraction of multiply charged ions can be more easily estimated and distinguished from incompletely cross-linked species. In comparison to other analytical methods such as gel electrophoresis, mass spectrometry offers higher sensitivity, better mass accuracy, and faster analysis time for the investigation of the cross-linked species, i.e., there is potential for using the strategy described herein for quality control purposes in the pharmaceutical industry. Moreover, the advantages of negative ion mode detection allow a fairly accurate determination of cross-linking yields for homomeric protein complexes with MALDI-MS. As shown previously, the amount of cross-linked complex can reflect the amount of complex in solution [52]. If the cross-linking yields are known (ideally close to 100%), chemical cross-linking and negative high-mass MALDI-MS could eventually be used to estimate binding affinities of homomeric protein complexes. This would require a number of cross-linking experiments using different subunit concentrations, similar to the ESI measurements carried out by Duckworth and coworkers for citrate synthase, and subsequent MALDI-MS analysis [7]. Additionally, the quantitative influence of ligands and buffer conditions on the stability of quaternary structures could be evaluated.

Conclusions

Negative ion mode high-mass MALDI-MS data of proteins and protein complexes are reported for the first time on a MALDI instrument equipped with a high-mass detector capable of detecting ions up to several 100 kDa. The negative ion mode detection of chemically cross-linked protein–protein complexes in MALDI-MS has been demonstrated to be less prone to formation of multiply charged species, and to provide lower background signals and generally cleaner spectra. We believe that the use of negative ion mode detection can improve the results of quantitative and qualitative studies of protein–protein interactions with MALDI-MS and chemical cross-linking and should be used complementary to positive ion mode, if available. The main disadvantage of negative ion mode is its absolute sensitivity, which is significantly lower than for positive ion mode. Consequently, species with concentrations close to the detection limit are more likely to be detected as cations than as anions. Sensitivity can be an important issue for the analysis of proteins with low abundance. However, in the case of cross-linking experiments, sufficient sample amounts are generally available. For three of the four selected examples, aldolase, GST, and GADPH, a good agreement between the expected amount of complex present in solution and the amount of stabilized complex detected in the mass spectra was obtained with negative ion mode. Investigating the stabilized complexes in negative ion mode can increase the chances of detecting the species with the highest oligomerization state, as demonstrated for GADPH.

Possible applications of chemical cross-linking and negative ion mode high-mass MALDI-MS for homomeric protein complexes include the investigation of complex stoichiometry and composition, as well as the determination of cross-linking yields. In the case of complete covalent stabilization of noncovalent complexes present in solution, K_D values could be estimated and ligands influencing the equilibrium composition in solution could be uncovered.

Sinapinic acid is an excellent matrix for the analysis of proteins and cross-linked protein complexes in both ion modes from a single sample preparation spot on the MALDI plate. This work clearly illustrated that MALDI mass spectra recorded in positive ion mode do not always reflect the solution state composition of the reaction mixture after chemical cross-linking. Consequently, negative ion mode measurements are recommended to complement positive ion mode data.

Acknowledgment

The authors acknowledge the Swiss National Science Foundation for financial supported of this work by grant no. 200020–124663. Additionally, the authors are thankful to Dr. Benoit Plêt and Dr. Alexis Nazabal (CovalX AG, Zurich, Switzerland) for fruitful discussions and providing access to the Bruker Reflex III instrument, Dr. Alfredo Ibanez for critically reading the manuscript, and the group of Professor Dr. D. Hilvert (ETH Zurich, Switzerland) for the opportunity to use the NanoDrop.

References

1. Goodsell, D.S., Olson, A.J.: Structural symmetry and protein function. *Annu. Rev. Biophys. Biomol. Struct.* **29**, 105–153 (2000)
2. van den Heuvel, R.H., Heck, A.J.: Native protein mass spectrometry: from intact oligomers to functional machineries. *Curr. Opin. Chem. Biol.* **8**, 519–526 (2004)
3. Heck, A.J.R., van den Heuvel, R.H.H.: Investigation of intact protein complexes by mass spectrometry. *Mass Spectrom. Rev.* **23**, 368–389 (2004)
4. Hernandez, H., Robinson, C.V.: Determining the stoichiometry and interactions of macromolecular assemblies from mass spectrometry. *Nat. Protocol.* **2**, 715–726 (2007)
5. Chitta, R.K., Rempel, D.L., Gross, M.L.: Determination of affinity constants and response factors of the noncovalent dimer of gramicidin by electrospray ionization mass spectrometry and mathematical modeling. *J. Am. Soc. Mass Spectrom.* **16**, 1031–1038 (2005)
6. Liu, J.J., Konermann, L.: Protein–protein binding affinities in solution determined by electrospray mass spectrometry. *J. Am. Soc. Mass Spectrom.* **22**, 408–417 (2011)
7. Ayed, A., Krutchinsky, A.N., Ens, W., Standing, K.G., Duckworth, H. W.: Quantitative evaluation of protein-protein and ligand-protein equilibria of a large allosteric enzyme by electrospray ionization time-of-flight mass spectrometry. *Rapid Commun. Mass Spectrom.* **12**, 339–344 (1998)
8. Farmer, T.B., Caprioli, R.M.: Assessing the multimeric states of proteins: Studies using laser desorption mass spectrometry. *Biol. Mass Spectrom.* **20**, 796–800 (1991)
9. Farmer, T.B., Caprioli, R.M.: Determination of protein–protein interactions by matrix-assisted laser desorption/ionization mass spectrometry. *J. Mass Spectrom.* **33**, 697–704 (1998)
10. Nazabal, A., Wenzel, R., Zenobi, R.: Immunoassays with direct mass spectrometric detection. *Anal. Chem.* **78**, 3562–3570 (2006)
11. Pimenova, T., Pereira, C.P., Schaer, D.J., Zenobi, R.: Characterization of high molecular weight multimeric states of human haptoglobin and hemoglobin-based oxygen carriers by high-mass MALDI MS. *J. Sep. Sci.* **32**, 1224–1230 (2009)
12. Budnik, B.A., Moyer, S.C., Pittman, J.L., Ivleva, V.B., Sommer, U., Costello, C.E., O'Connor, P.B.: High pressure MALDI-FTMS: Implications for proteomics. *Int. J. Mass Spectrom.* **234**, 203–212 (2004)
13. O'Connor, P.B., Costello, C.E.: A high pressure matrix-assisted laser desorption/ionization fourier transform mass spectrometry ion source for thermal stabilization of labile biomolecules. *Rapid Commun. Mass Spectrom.* **15**, 1862–1868 (2001)
14. Zhou, J., Lee, T.: Charge state distribution shifting of protein ions observed in matrix-assisted laser desorption ionization mass spectrometry. *J. Am. Soc. Mass Spectrom.* **6**, 1183–1189 (1995)
15. Kononikhin, A.S., Nikolaev, E.N., Frankevich, V., Zenobi, R.: Letter: Multiply charged ions in matrix-assisted laser desorption/ionization generated from electrosprayed sample layers. *Eur. J. Mass Spectrom.* **11**, 257–259 (2005)
16. Frankevich, V., Zhang, J., Dashtiev, M., Zenobi, R.: Production and fragmentation of multiply charged ions in "electron-free" matrix-assisted laser desorption/ionization. *Rapid Commun. Mass Spectrom.* **17**, 2343–2348 (2003)
17. Frankevich, V.E., Zhang, J., Friess, S.D., Dashtiev, M., Zenobi, R.: Role of electrons in laser desorption/ionization mass spectrometry. *Anal. Chem.* **75**, 6063–6067 (2003)
18. Gorshkov, M.V., Frankevich, V.E., Zenobi, R.: Characteristics of photoelectrons emitted in matrix-assisted laser desorption/ionization Fourier transform ion cyclotron resonance experiments. *Eur. J. Mass Spectrom.* **8**, 67–69 (2002)
19. Jorgensen, T.J.D., Bojesen, G., Rahbek-Nielsen, H.: The proton affinities of seven matrix-assisted laser desorption/ionization matrices correlated with the formation of multiply charged ions. *Eur. J. Mass Spectrom.* **4**, 39–45 (1998)
20. Karas, M., Kruger, R.: Ion formation in MALDI: The cluster ionization mechanism. *Chem. Rev.* **103**, 427–440 (2003)
21. Tsai, S.T., Chen, C.W., Huang, L.C.L., Huang, M.C., Chen, C.H., Wang, Y.S.: Simultaneous mass analysis of positive and negative ions using a dual-polarity time-of-flight mass spectrometer. *Anal. Chem.* **78**, 7729–7734 (2006)
22. Alves, S., Fournier, F., Afonso, C., Wind, F., Tabet, J.C.: Gas-phase ionization/desolvation processes and their effect on protein charge state distribution under matrix-assisted laser desorption/ionization conditions. *Eur. J. Mass Spectrom.* **12**, 369–383 (2006)
23. Yau, P.Y., Dominic Chan, T.W., Cullis, P.G., Colburn, A.W., Derrick, P.J.: Threshold fluences for production of positive and negative ions in matrix-assisted laser desorption/ionisation using liquid and solid matrices. *Chem. Phys. Lett.* **202**, 93–100 (1993)
24. Dashtiev, M., Wafler, E., Rohling, U., Gorshkov, M., Hillenkamp, F., Zenobi, R.: Positive and negative analyte ion yield in matrix-assisted laser desorption/ionization. *Int. J. Mass Spectrom.* **268**, 122–130 (2007)
25. Karas, M., Glückmann, M., Schäfer, J.: Ionization in matrix-assisted laser desorption/ionization: singly charged molecular ions are the lucky survivors. *J. Mass Spectrom.* **35**, 1–12 (2000)
26. Knochenmuss, R., Stortelder, A., Breuker, K., Zenobi, R.: Secondary ion–molecule reactions in matrix-assisted laser desorption/ionization. *J. Mass Spectrom.* **35**, 1237–1245 (2000)
27. Knochenmuss, R.: A quantitative model of ultraviolet matrix-assisted laser desorption/ionization including analyte ion generation. *Anal. Chem.* **75**, 2199–2207 (2003)
28. Knochenmuss, R.: A quantitative model of ultraviolet matrix-assisted laser desorption/ionization. *J. Mass Spectrom.* **37**, 867–877 (2002)
29. Knochenmuss, R.: A bipolar rate equation model of MALDI primary and secondary ionization processes, with application to positive/negative analyte ion ratios and suppression effects. *Int. J. Mass Spectrom.* **285**, 105–113 (2009)
30. Jaskolla, T.W., Karas, M.: Compelling evidence for lucky survivor and gas phase protonation: The unified MALDI analyte protonation mechanism. *J. Am. Soc. Mass Spectrom.* **22**, 976–988 (2011)
31. Liu, B.H., Lee, Y.T., Wang, Y.S.: Incoherent production reactions of positive and negative ions in matrix-assisted laser desorption/ionization. *J. Am. Soc. Mass Spectrom.* **20**, 1078–1086 (2009)
32. Hillenkamp, F., Nazabal, A., Roehling, U., Wenzel, R.: Method for analyzing ions of high mass in time-of-flight mass spectrometer, involves applying potential difference between front and back sides of electron multiplier to multiply number of electrons. WO2009086642-A1 WOCH000007 04 Jan 2008
33. Lomant, A.J., Fairbanks, G.: Chemical probes of extended biological structures: Synthesis and properties of the cleavable protein cross-linking reagent [35S]Dithiobis(succinimidyl propionate). *J. Mol. Biol.* **104**, 243–261 (1976)
34. Bich, C., Mädler, S., Chiesa, K., DeGiacomo, F., Bogliotti, N., Zenobi, R.: Reactivity and applications of new amine reactive cross-linkers for mass spectrometric detection of protein-protein complexes. *Anal. Chem.* **82**, 172–179 (2010)
35. Svatos, A., Shroff, R.: Proton sponge: A novel and versatile MALDI matrix for the analysis of metabolites using mass spectrometry. *Anal. Chem.* **81**, 7954–7959 (2009)
36. Kirpekar, F., Nordhoff, E., Kristiansen, K., Roepstorff, P., Lezius, A., Hahner, S., Karas, M., Hillenkamp, F.: Matrix-assisted laser-desorption ionization mass spectrometry of enzymatically synthesized RNA up to 150 kDa. *Nucleic Acids Res.* **22**, 3866–3870 (1994)
37. Xu, C.F., Lu, Y., Ma, J., Mohammadi, M., Neubert, T.A.: Identification of phosphopeptides by MALDI Q-TOF MS in positive and negative ion modes after methyl esterification. *Mol. Cell. Proteomics* **4**, 809–818 (2005)
38. Gao, J., Cassady, C.J.: Negative ion production from peptides and proteins by matrix-assisted laser desorption/ionization time-of-flight mass spectrometry. *Rapid Commun. Mass Spectrom.* **22**, 4066–4072 (2008)
39. Kaltashov, I.A., Mohimen, A.: Estimates of protein surface areas in solution by electrospray ionization mass spectrometry. *Anal. Chem.* **77**, 5370–5379 (2005)
40. van Breukelen, B., Barendregt, A., Heck, A.J.R., van den Heuvel, R.H. H.: Resolving stoichiometries and oligomeric states of glutamate synthase protein complexes with curve fitting and simulation of electrospray mass spectra. *Rapid Commun. Mass Spectrom.* **20**, 2490–2496 (2006)
41. Knochenmuss, R., Zenobi, R.: MALDI ionization: The role of in-plume processes. *Chem. Rev.* **103**, 441–452 (2003)
42. Breuker, K., Knochenmuss, R., Zenobi, R.: Gas-phase basicities of deprotonated matrix-assisted laser desorption/ionization matrix molecules. *Int. J. Mass Spectrom.* **184**, 25–38 (1999)
43. Jones, C.M., Bernier, M., Carson, E., Colyer, K.E., Metz, R., Pawlow, A., Wischow, E.D., Webb, I., Andriole, E.J., Poutsma, J.C.: Gas-phase acidities of the 20 protein amino acids. *Int. J. Mass Spectrom.* **267**, 54–62 (2007)

44. Knochenmuss, R.: Ion formation mechanisms in UV-MALDI. *Analyst* **131**, 966–986 (2006)
45. Zhong, F., Zhao, S.: A study of factors influencing the formation of singly charged oligomers and multiply charged monomers by matrix-assisted laser desorption/ionization mass spectrometry. *Rapid Commun. Mass Spectrom.* **9**, 570–572 (1995)
46. Brunelle, A., Chaurand, P., Dellanegra, S., Lebeyec, Y., Baptista, G.B.: Surface secondary-electron and secondary-ion emission induced by large molecular ion impacts. *Int. J. Mass Spectrom. Ion Process* **126**, 65–73 (1993)
47. Beuhler, R.J., Friedman, L.: Threshold studies of secondary electron emission induced by macro-ion impact on solid surfaces. *Nucl. Instrum. Meth.* **170**, 309–315 (1980)
48. Coeck, S., Beck, M., DelaurÈ, B., Golovko, V.V., Herbane, M., Lindroth, A., Kopecky, S., Kozlov, V.Y., Kraev, I.S., Phalet, T., Severijns, N.: Microchannel plate response to high-intensity ion bunches. *Nucl. Instrum. Meth. Phy. Res. Section A: Accelerators, Spectrometers, Detectors, and Associated Equipment* **557**, 516–522 (2006)
49. Tolan, D.R., Schuler, B., Beernink, P.T., Jaenicke, R.: Thermodynamic analysis of the dissociation of the aldolase tetramer substituted at one or both of the subunit interfaces. *Biol. Chem.* **384**, 1463–1471 (2003)
50. Lim, K., Ho, J.X., Keeling, K., Gilliland, G.L., Ji, X., Ruker, F., Carter, D.C.: Three-dimensional structure of Schistosoma japonicum glutathione S-transferase fused with a six-amino acid conserved neutralizing epitope of gp41 from HIV. *Protein Sci.* **3**, 2233–2244 (1994)
51. Hoagland Jr., V.D., Teller, D.C.: Influence of substrates on the dissociation of rabbit muscle D-glyceraldehyde 3-phosphate dehydrogenase. *Biochemistry* **8**, 594–602 (1969)
52. Mädler, S., Seitz, M., Robinson, J., Zenobi, R.: Does chemical cross-linking with NHS esters reflect the chemical equilibrium of protein-protein noncovalent interactions in solution? *J. Am. Soc. Mass Spectrom.* **21**, 1775–1783 (2010)